

# A Framework for Discrete-Time Preview Control

Please change to  
andrew\_hazell@fmail.co.uk

*The purpose of this paper is to provide a set of synthesis and design tools for a wide class of  $\mathcal{H}_2$  preview control systems. A generic preview design problem, which features both previewable and nonpreviewable disturbances, is embedded in a standard generalized regulator framework. Preview regulation is accomplished by a two-degrees-of-freedom output-feedback controller. A number of theoretical issues are studied, including the efficient solution of the standard  $\mathcal{H}_2$  full-information Riccati equation and the efficient evaluation of the full-information preview gain matrices. The full-information problem is then extended to include the efficient implementation of the output-feedback controller. The synthesis of feedforward controllers with preview is analyzed as a special case—this problem is of interest to designers who wish to introduce preview as a separate part of a system design. The way in which preview reduces the  $\mathcal{H}_2$ -norm of the closed-loop system is analyzed in detail. Closed-loop norm reduction formulas provide a systematic way of establishing how much preview is required to solve a particular problem, and determine when extending the preview horizon will not produce worthwhile benefits. The paper concludes with a summary of the main features of preview control, as well as some controller design insights. New application examples are introduced by reference.*

[DOI: 10.1115/1.4000810]

Please change post code  
to: OX1 3PJ

**A. J. Hazell**  
e-mail: andrew\_hazell@fmail.co.uk

**D. J. N. Limebeer<sup>1</sup>**  
e-mail: david.limebeer@eng.ox.ac.uk

Department of Engineering Science,  
University of Oxford,  
Parks Road,  
Oxford OX2 7DQ

## 1 Introduction

There are many situations in which reference signals or future disturbances are “previewable.” Optimal preview control is concerned with designing controllers that exploit previewed information in order to achieve performance levels that are superior to those achievable using current information alone. This paper considers the generic preview synthesis problem illustrated in Fig. 1, which comprises a two-degrees-of-freedom controller and both previewed disturbances/references ( $r$ ) and unpreviewed disturbances ( $w$ ). An  $\mathcal{H}_2$ -optimal solution to this controller synthesis problem is provided that requires only low-dimensional computations and low-dimensional Riccati equation solutions, and leads to a controller whose high-dimensional component is a finite impulse response (FIR) filter; the efficient implementation of FIR filters is well known in the signal processing literature. The low-dimensional solution to the problem described in Fig. 1 derives from the fact that the states of the (high-dimensional) delay line can be reconstructed by making a copy of  $\Phi$  in the controller. The objective of this paper is to provide a framework for synthesizing preview controllers for any problem that fits into the framework illustrated in Fig. 1. In addition, we aim to provide some general insights into the design of preview controllers and a method for assessing the effectiveness of preview in terms of the achievable  $\mathcal{H}_2$ -norm reduction.

One of the first papers to recognize the importance of preview control is Ref. [1], in which three preview control models are described. In the third of these models, open-loop optimal preview controls are found using dynamic programming. The earliest applied work on preview control dates back to that in Ref. [2], where the Wiener filter theory was used to design an active suspension with road preview. This solution was not implementable, as it required the transfer function from the previewed path to the vehicle’s acceleration to be unstable. Much of the subsequent work on preview tracking has its origins from the thesis done by Tomizuka [3], in which the preview control task is cast in a discrete-

time linear quadratic regulator framework by augmenting the plant dynamics with a delay line model. In this formulation, the number of states grows in direct proportion to the preview length and so a direct solution of the corresponding Riccati equations becomes computationally infeasible for long preview lengths. Tomizuka [3] presented an efficient recursive method for solving these large equations. A continuous-time version of a linear quadratic (LQ) preview control problem is studied in Ref. [4], while a continuous-time preview control problem is given a stochastic interpretation in Ref. [5].

In the context of the early literature, Ref. [6] provides a good overview of an output-feedback preview-tracking problem with reference noise. This paper also summarizes many of the basic properties of preview feedback controllers. Motivated by a process control problem, another previewable command reference variant, the so-called proportional, integral, derivative, preview (PIDP) controller is studied in Ref. [7] in a LQ optimal control framework. A closely associated feedforward problem is studied in Ref. [8]. Other schemes for computing a feedforward-only controller is given in Refs. [9,10]. The vehicle suspension preview problem by Bender [2] is revisited in Ref. [11] in a discrete-time command preview framework. The preview suspension problem has attracted the attention of several practitioners in the more recent literature; examples include Refs. [12–15].

We will use the problem formulation in Fig. 1 as a basis for the results presented here. A solution will be derived by formulating the problem in a generalized regulator framework [16,17], and then finding efficient solutions to the resulting high-dimension Riccati equations. Contributions made by this paper include:

- an efficient method for finding the  $\mathcal{H}_2$ -norm of the closed-loop system
- a method for evaluating the benefit of preview
- a low-order output-feedback controller implementation
- an analysis of the generic properties of preview controllers

Figure 2 illustrates a simple example that may be used to highlight the benefit of preview, the broad structure of the controller, and the effect of preview on the achievable  $\mathcal{H}_2$ -norm of the closed-loop system. The preview action arises from the delay line  $\Phi$ . The input to the controller is  $r$ , which is the future value of the

<sup>1</sup>Corresponding author.

Contributed by Dynamic Systems Division of ASME for publication in the JOURNAL OF DYNAMIC SYSTEMS, MEASUREMENT, AND CONTROL. Manuscript received August 22, 2007; final manuscript received June 18, 2009; published online xxxxx-xxxxx-xxxxx. Editor: J. Karl Hedrick.

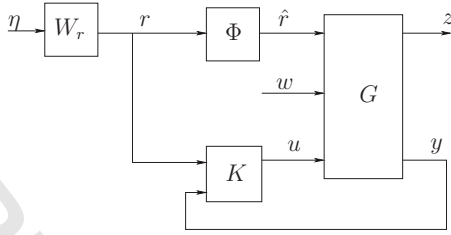


**Fig. 1** A generalized regulator problem with both previewable and nonpreviewable disturbances. The transfer function  $G$  is the system to be controlled,  $K$  is the controller to be synthesized, and  $\Phi = \mathcal{Z}^{-N}$  is an  $N$ -step delay line (where  $\mathcal{Z}$  is the  $\mathcal{Z}$ -transform variable). The disturbance  $w$  is not previewable, the control and measurement signals are  $u$  and  $y$ , respectively,  $\hat{r}$  is the previewable disturbance, and  $r$  is the future value of  $\hat{r}$ . The filter  $W_r$  is used to model the expected frequency content of  $r$ .

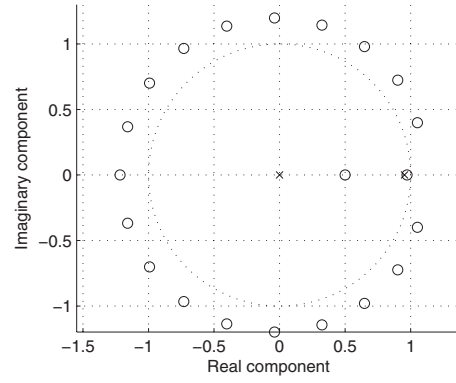


**Fig. 3** Pole-zero plot of the  $\mathcal{H}_2$ -optimal  $K(\mathcal{Z})$  for the case where  $c_z = 1.05$ ,  $G(\mathcal{Z}) = (\mathcal{Z} - c_z)/(\mathcal{Z} - 0.5)$  and  $N = 20$ . Crosses represent the poles and circles represent the zeros.

reference, and  $K$  is chosen so as to ensure that  $e$  is “small,” and hence the plant output follows  $\Phi r$  as closely as possible. Define the error system

$$E(\mathcal{Z}) = G(\mathcal{Z})K(\mathcal{Z}) - \Phi(\mathcal{Z})$$

and assume that  $G(\mathcal{Z})$  is stable; in the case that  $G(\mathcal{Z})$  is unstable, it could be replaced by  $\hat{G}(\mathcal{Z}) = G(\mathcal{Z})(1 - G(\mathcal{Z})K_f(\mathcal{Z}))^{-1}$  in which  $K_f(\mathcal{Z})$  is a stabilizing feedback controller. Providing that  $G(\mathcal{Z})$  has all its zeros inside the unit circle, perfect tracking ( $E(\mathcal{Z}) = 0$ ) may be achieved by simply setting  $K(\mathcal{Z}) = G(\mathcal{Z})^{-1}\Phi(\mathcal{Z})$ . However, if  $G(\mathcal{Z})$  is a nonminimum phase (NMP), then such a  $K(\mathcal{Z})$  is not internally stabilizing and a controller must be found that recognizes the limits imposed by NMP zeros on the achievable tracking performance.

For the case where  $G(\mathcal{Z})$  is an arbitrary stable rational transfer function having a single real NMP zero at  $c_z$ , the  $\mathcal{H}_2$ -optimal controller is easily found. Our objective is to find an internally stabilizing  $K(\mathcal{Z})$  such that  $\|E(\mathcal{Z})\|_2$  is minimized.

The following inner-outer factorization may be performed:

$$G(\mathcal{Z}) = G_o(\mathcal{Z})G_i(\mathcal{Z})$$

where

$$G_i(\mathcal{Z}) = \frac{\mathcal{Z} - c_z}{1 - \mathcal{Z}c_z}$$

We can write  $E(\mathcal{Z}) = (\tilde{K}(\mathcal{Z}) - \Phi(\mathcal{Z})G_i(\mathcal{Z}^{-1}))G_o(\mathcal{Z})$  in which  $\tilde{K}(\mathcal{Z}) = K(\mathcal{Z})G_o(\mathcal{Z})$  with  $G_i(\mathcal{Z}^{-1})G_i(\mathcal{Z}) = 1$ . The optimal controller is found by setting  $K(\mathcal{Z}) = (\Phi(\mathcal{Z})G_i(\mathcal{Z}^{-1}))_+ G_o^{-1}(\mathcal{Z})$ , where  $(\cdot)_+$  denotes the stable projection [18,16]. It follows by direct calculation that:

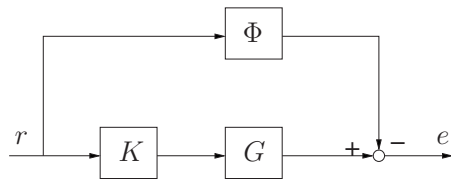


**Fig. 2** A simple single-input-single-output (SISO) open-loop preview-tracking problem. The transfer function  $\Phi = \mathcal{Z}^{-N}$  is an  $N$ -step delay,  $G$  is the plant to be controlled, and  $K$  is a feedforward controller. The signal  $r$  is the future value of the reference, and  $e$  is the tracking error.

$$K(\mathcal{Z}) = \underbrace{G_o(\mathcal{Z})^{-1}}_{\text{IIR}} \underbrace{\left( -c_z^{-1}\mathcal{Z}^{-N} + (1 - c_z^{-2})c_z \sum_{i=1}^N (\mathcal{Z}^{-N}/c_z^i) \right)}_{\text{FIR}}$$

and that

$$\|E(\mathcal{Z})\|_2 = \frac{1}{|c_z^{N+1}|} \sqrt{c_z^2 - 1} \quad (1)$$

Since  $\|E(\mathcal{Z})\|_2 \rightarrow 0$  as  $N \rightarrow \infty$ , we conclude that in this example, preview action can overcome completely the tracking limitation imposed by the NMP zero. The optimal controller contains a high-order FIR part and a low-order infinite impulse response (IIR) part, where the preview action comes from the FIR part. The dynamics of the FIR block is fully specified by the RHP zero  $c_z$  and the preview length  $N$ . The fact that the high-order part of the controller is a FIR leads to an efficient hardware implementation.

A pole-zero plot of the optimal controller is given in Fig. 3 for the case where  $c_z = 1.05$ ,  $G_o(\mathcal{Z}) = (1 - \mathcal{Z}c_z)/(\mathcal{Z} - 0.5)$ , and  $N = 20$ . Notice the almost pole-zero cancellation on the real axis. In the limit  $N \rightarrow \infty$ , cancellation occurs. This simple preview problem highlights several important features that will be carried over into the more complex problem treated in this paper. In particular:

- (1) The preview action is captured in a FIR block having order  $N$ .
- (2) The remainder of the controller (the IIR part) has order equal to the plant order.
- (3) The preview length ( $N$ ) required to achieve 95% (for example) of the maximum norm reduction due to preview, is affected by the position of NMP zeros.

Point 3 merits further discussion. A central tenet of this paper is that the preview length could be sufficiently large that solution of the associated discrete algebraic Riccati equation (DARE) is computationally intractable. However, it might be argued that it is never necessary to use a large preview length because one could simply reduce the sampling rate until  $N$  becomes sufficiently small. In Ref. [19], an example similar to Fig. 2 is treated in continuous-time, and it is found that the required preview time is purely a function of the position of the continuous-time zero. The discrete-time equivalent of this result is: for a given performance improvement, the preview time  $NT_s$  (where  $T_s$  represents the sample time) is determined by the position of the continuous-time zero. This fact can be seen by considering the effect of  $T_s$  on the magnitude of  $c_z$  in Ref. [1]. Typically, the sampling rate is determined by the frequency at which tracking or disturbance rejection is required, and also by the frequency of any unstable poles [20]. It therefore follows that a combination of low-frequency zeros

(which impose a large  $NT_s$ ) and higher frequency performance specifications or unstable poles (which impose a low  $T_s$ ) would lead unavoidably to a large preview length ( $N$ ). At this stage, the reader might be left with the impression that preview is of no benefit for minimum phase (MP) systems. However, as an example, it can be shown that the minimum achievable  $\mathcal{H}_2$ -norm of the transfer function

$$\begin{bmatrix} E(\mathcal{Z}) \\ \rho K(\mathcal{Z}) \end{bmatrix}$$

is reduced by preview action, even when  $G(\mathcal{Z})$  is MP. By adding the additional term  $\rho K(\mathcal{Z})$  into the optimization, we are effectively penalizing the magnitude of the control action. In general, a large  $\rho$  leads to a slow response and so a large  $N$  is required in order to get the full benefit from preview action. A detailed analysis of the effects of preview on systems of this form is given in Ref. [21] (chapter 4).

The paper is structured as follows: Preliminaries and some standard notation is given in Sec. 2. A state-space description of the generalized regulator problem with both previewable and nonpreviewed exogenous disturbances is derived in Sec. 3. The solution of this problem, which is illustrated in Fig. 1, is the central focus of the paper. Following a summary of the general theory, the full-information preview control problem is solved in Sec. 4. The results are mainly concerned with efficient algorithms for solving the  $\mathcal{H}_2$  full-information Riccati equation, and the evaluation of the full-information feedback gain matrix. The solution of the output-feedback preview problem is given in Sec. 5. The output-feedback controller involves a combination of a state estimator, and the solution to the full-information problem. An efficient controller synthesis is also given in this section. The effect of preview in reducing the  $\mathcal{H}_2$ -norm of the closed-loop system is analyzed in Sec. 6. The special case of feedforward control with preview is analyzed in Sec. 7. A summary of the main features of preview controllers, as well as some design insights, are given in Sec. 8. The conclusions are given in Sec. 9.

## 2 Notation and Preliminaries

We will make use of discrete-time state-space models of the form

$$x(k+1) = Ax(k) + Bu(k)$$

$$y(k) = Cx(k) + Du(k)$$

in which  $k$  is the time index;  $x(k)$  is a vector of state variables;  $u(k)$  is a vector of inputs;  $y(k)$  is a vector of outputs; and  $A$ ,  $B$ ,  $C$ , and  $D$  are appropriately dimensioned real matrices. Signals will sometimes be represented by omitting the time index, e.g.,

$$x = \{x(k)\}_{-\infty}^{\infty}$$

When transfer functions are associated with these models, they are computed using

$$G(\mathcal{Z}) = C(\mathcal{Z}I - A)^{-1}B + D$$

in which  $\mathcal{Z}$  is the  $Z$ -transform variable. We will also use the shorthand notation

$$G(\mathcal{Z}) \stackrel{s}{=} \begin{bmatrix} A & B \\ C & D \end{bmatrix} \quad (2)$$

The transfer function  $G(\mathcal{Z})$  will be abbreviated by  $G$  when no confusion will occur.

The (lower) linear fractional transformation of the transfer-function matrices

$$P = \begin{bmatrix} P_{11} & P_{12} \\ P_{21} & P_{22} \end{bmatrix}$$

and  $K$  will be written as  $F_l(P, K)$ , where

$$F_l(P, K) = P_{11} + P_{12}K(I - P_{22}K)^{-1}P_{21} \quad 200$$

The trace of a matrix will be denoted  $\text{Tr}\{A\}$ . 201

The  $\mathcal{H}_2$ -norm of a transfer function  $G(\mathcal{Z})$  will be denoted by  $\|G(\mathcal{Z})\|_2$ , and is defined by 202  
203

$$\|G(\mathcal{Z})\|_2^2 = \frac{1}{2\pi} \int_{-\pi}^{\pi} \text{Tr}\{G(e^{j\theta})' G(e^{j\theta})\} d\theta \quad 204$$

If  $G$  has the realization (2), with  $A$  assumed stable, and  $X$  is a matrix, which satisfies 205  
206

$$X = A'XA + C'C \quad 207$$

then 208

$$\|G(\mathcal{Z})\|_2^2 = \text{Tr}\{B'XB + D'D\} \quad (3) \quad 209$$

A transfer function that maps signal  $a$  to signal  $b$  will be denoted  $T_{a \rightarrow b}$ . 210  
211

An  $m \times p$ -dimensional zero matrix will be denoted as  $0_{m \times p}$  and an  $n$ -dimensional identity matrix will be written as  $I_n$ . The shorthand  $0_m = 0_{m \times m}$  will also be used. 212  
213  
214

The complex conjugate transpose of  $A$  will be denoted  $A'$  and  $n$ -dimensional real vectors are denoted  $\mathbb{R}^n$ . 215  
216

## 3 Problem Formulation

The  $\mathcal{H}_2$ -optimal preview controller is defined to be the  $K$  that minimizes  $\|T_{v \rightarrow z}\|_\infty$ , where  $v = [\eta' \ w']'$  with  $w$ ,  $\eta$ , and  $z$  defined in Fig. 1. In other words, we wish to choose  $K$ , which minimizes  $\|F_l(P, K)\|_2$ , where  $P$  is the mapping 217  
218  
219  
220  
221

$$\begin{bmatrix} z \\ y \\ r \end{bmatrix} = \begin{bmatrix} P_{11} & P_{12} \\ P_{21} & P_{22} \end{bmatrix} \begin{bmatrix} \eta \\ w \\ u \end{bmatrix} \quad 222$$

The signals satisfy:  $w(k) \in \mathbb{R}^{l_w}$ ,  $r(k) \in \mathbb{R}^{l_r}$ ,  $\eta(k) \in \mathbb{R}^{l_r}$ ,  $v(k) \in \mathbb{R}^{l_r}$  (i.e.,  $l = l_r + l_w$ ),  $u(k) \in \mathbb{R}^m$ ,  $y(k) \in \mathbb{R}^{q_s}$ , and  $z(k) \in \mathbb{R}^p$ . Also,  $q$  is defined as  $q = q_s + l_r$ . The  $N$ -step delay line  $\Phi$  has the realization 223  
224  
225

$$\Phi(\mathcal{Z}) = \mathcal{Z}^{-N} I_{l_r} \stackrel{s}{=} \begin{bmatrix} A_p & B_p \\ C_p & 0_{l_r \times l_r} \end{bmatrix} \quad 226$$

with  $A_p$ ,  $B_p$  and  $C_p$  defined by 227

$$A_p = \begin{bmatrix} 0_{l_r} & I_{l_r} & \cdots & 0_{l_r} \\ \vdots & \vdots & & \vdots \\ 0_{l_r} & 0_{l_r} & \cdots & I_{l_r} \\ 0_{l_r} & 0_{l_r} & \cdots & 0_{l_r} \end{bmatrix} \quad 228$$

and 229

$$B_p = \begin{bmatrix} 0_{(N-1)l_r \times l_r} \\ I_{l_r} \end{bmatrix}, \quad C_p = \begin{bmatrix} I_{l_r} & 0_{l_r \times (N-1)l_r} \end{bmatrix} \quad 230$$

where  $N$  represents the number of preview steps and  $A_p \in \mathbb{R}^{Nl_r \times Nl_r}$ . Without loss of generality the square transfer function  $W_r$  is assumed to be outer [16,17], with realization 231  
232  
233

$$W_r \stackrel{s}{=} \begin{bmatrix} A_r & B_r \\ C_r & D_r \end{bmatrix} \quad 234$$

where  $A_r \in \mathbb{R}^{n_r \times n_r}$ . Also without loss of generality [16], the plant is assumed to have the realization 235  
236

$$G \stackrel{s}{=} \begin{bmatrix} A_g & B_{1gr} & B_{1gw} & B_{2g} \\ C_{1g} & D_{11gr} & D_{11gw} & D_{12} \\ C_{2g} & D_{21gr} & D_{21gw} & 0 \end{bmatrix} \quad 237$$

where  $A_g \in \mathbb{R}^{n_g \times n_g}$ . 238

The transfer function from  $\eta$  to  $\begin{bmatrix} \hat{r} \\ r \end{bmatrix}$  has realization 239

$$\begin{bmatrix} A_d & B_d \\ C_{d1} & 0 \\ C_{d2} & D_r \end{bmatrix} = \begin{bmatrix} A_p & 0 \\ C_p & 0 \\ 0 & C_r & D_r \end{bmatrix}$$

Font size too large. Both horizontal and vertical should be the same.

$$F_0 = -\bar{R}^{-1}(B_2'XB_1 + D_{12}'D_{11}) \quad 270$$

The resulting closed-loop norm is given by 271

$$\|F_1(P_{FI}, K_{FI})\|_2^2 = \text{Tr}\{(D_{11} + D_{12}F_0)'(D_{11} + D_{12}F_0) + (B_1 \quad 272$$

$$+ B_2F_0)'X(B_1 + B_2F_0)\} \quad 273$$

240

241 and so the generalized plant  $P$  has realization

$$P = \begin{matrix} \begin{matrix} n_g & n_l+n_r & l_r & l_w & m \\ \leftrightarrow & \leftrightarrow & \leftrightarrow & \leftrightarrow & \leftrightarrow \\ \begin{matrix} n_g \downarrow \\ n_l+n_r \downarrow \\ p \downarrow \\ q \downarrow \\ l_r \downarrow \end{matrix} \end{matrix} \begin{bmatrix} A_g & B_{1gr}C_{d1} & 0 & B_{1gw} & B_{2g} \\ 0 & A_d & B_d & 0 & 0 \\ C_{1g} & D_{11gr}C_{d1} & 0 & D_{11gw} & D_{12} \\ C_{2g} & D_{21gr}C_{d1} & 0 & D_{21gw} & 0 \\ 0 & C_{d2} & D_r & 0 & 0 \end{bmatrix} \end{matrix} \quad (4)$$

242

$$= \begin{bmatrix} A & B_1 & B_2 \\ C_1 & D_{11} & D_{12} \\ C_2 & D_{21} & 0 \end{bmatrix} \quad (5)$$

243

244 The  $A$ -matrix in Eq. (5) satisfies  $A \in \mathbb{R}^{n \times n}$  with  $n = n_g + n_l + n_r$ .

## 245 4 Full-Information Control Problem

246 **4.1 Standard Theory.** We begin with a brief summary of the  
247 discrete-time, linear time-invariant perfect information control  
248 problem [16], which has plant description

$$P_{FI} = \begin{matrix} \begin{matrix} n & l & m \\ \leftrightarrow & \leftrightarrow & \leftrightarrow \\ \begin{matrix} n \downarrow \\ p \downarrow \\ n \downarrow \\ l \downarrow \end{matrix} \end{matrix} \begin{bmatrix} A & B_1 & B_2 \\ C_1 & D_{11} & D_{12} \\ I & 0 & 0 \\ 0 & I & 0 \end{bmatrix} \end{matrix}$$

249

250 and which satisfies the following standard assumptions:

251 (A1)  $(A, B_2)$  is stabilizable.

252 (A2)  $D_{12}'D_{12} > 0$ .

253 (A3)  $\text{rank} \begin{bmatrix} A - e^{j\theta}I & B_2 \\ C_1 & D_{12} \end{bmatrix} = n + m, \quad \forall \theta \in (-\pi, \pi]$ .

254 We would like to find the internally stabilizing controller  $K_{FI}$ ,  
255 which minimizes  $\|F_1(P_{FI}, K_{FI})\|_2$ . First, define

$$\bar{R} = D_{12}'D_{12} + B_2'XB_2 \quad (6)$$

$$F_2 = -\bar{R}^{-1}(B_2'XA + D_{12}'C_1) \quad (7)$$

$$A_c = A + B_2F_2 \quad (8)$$

259 In Ref. [17] it is shown that if (A1)–(A3) are satisfied, then  
260 there exists a solution  $X$  to the DARE

$$X = A'XA - F_2'\bar{R}F_2 + C_1'C_1 \quad (9)$$

262 such that

$$X \geq 0 \quad (10)$$

$$A_c \text{ is asymptotically stable.} \quad (11)$$

265 A matrix  $X$  satisfying Eqs. (9) and (11) is said to be *stabilizing*.  
266 The internally stabilizing, full-information  $\mathcal{H}_2$ -optimal control-  
267 ler is then given by

$$K_{FI} = [F_2 \quad F_0] \quad (12)$$

269 with

## 4.2 Efficient Computation of the Full-Information Controller. 274

In this section, we will find an efficient solution for the DARE in Eq. (9) for the plant described in Sec. 3. First, we decompose Eq. (9) into an  $n_g$ -dimensional DARE, an  $n_l + n_r$ -dimensional discrete Lyapunov equation, and an  $n_g \times n_l + n_r$ -dimensional Stein equation. We then give an efficient solution to the Stein equation, and show how this leads to an efficient method for computing the full-information controller.

Lemma 4.1 (decomposition of the DARE). Let  $X$  be the unique stabilizing and non-negative solution to the DARE in Eq. (9), and partition  $X$  as

$$X = \begin{matrix} \begin{matrix} n_g & n_l+n_r \\ \leftrightarrow & \leftrightarrow \\ \begin{matrix} n_g \downarrow \\ n_l+n_r \downarrow \end{matrix} \end{matrix} \begin{bmatrix} X_{gg} & X_{gd} \\ X_{gd}' & X_{dd} \end{bmatrix} \end{matrix}$$

then  $X_{gg}$  is the unique stabilizing and non-negative solution to the DARE 286  
287

$$X_{gg} = A_g'X_{gg}A_g - F_{2g}'\bar{R}F_{2g} + C_{1g}'C_{1g} \quad (13) \quad 288$$

where 289

$$F_{2g} = -\bar{R}^{-1}(B_{2g}'X_{gg}A_g + D_{12}'C_{1g}) \quad (14) \quad 290$$

in which  $\bar{R}$  may be computed from 291

$$\bar{R} = B_{2g}'X_{gg}B_{2g} + D_{12}'D_{12} \quad (15) \quad 292$$

Furthermore,  $X_{gd}$  and  $X_{dd}$  are the unique solutions to 293

$$X_{gd} = SC_{d1} + A_c'X_{gd}A_d \quad (16) \quad 294$$

$$X_{dd} = A_d'X_{dd}A_d + Q \quad (17) \quad 295$$

with 296

$$S = A_g'X_{gg}B_{1gr} + F_{2g}'B_{2g}'X_{gg}B_{1gr} + F_{2g}'D_{12}'D_{11gr} + C_{1g}'D_{11gr} \quad 297$$

$$A_{cg} = A_g + B_{2g}F_{2g} \quad 298$$

$$F_{2d} = -\bar{R}^{-1}(B_{2g}'X_{gd}A_d + B_{2g}'X_{gg}B_{1gr}C_{d1} + D_{12}'D_{11gr}C_{d1}) \quad 299$$

$$Q = C_{d1}'B_{1gr}'X_{gg}B_{1gr}C_{d1} + A_d'X_{gd}'B_{1gr}C_{d1} + C_{d1}'B_{1gr}'X_{gd}A_d - F_{2d}'\bar{R}F_{2d} \quad 300$$

$$+ C_{d1}'D_{11gr}D_{11gr}C_{d1} \quad 301$$

Proof. First, partition Eq. (7) conformably with  $X$  302

$$F_2 = -\bar{R}^{-1} \begin{bmatrix} B_{2g}' & 0 \end{bmatrix} \begin{bmatrix} X_{gg} & X_{gd} \\ X_{gd}' & X_{dd} \end{bmatrix} \begin{bmatrix} A_g & B_{1gr}C_{d1} \\ 0 & A_d \end{bmatrix} \quad 303$$

$$+ D_{12}' \begin{bmatrix} C_{1g} & D_{11gr}C_{d1} \end{bmatrix} \quad 304$$

$$= -\bar{R}^{-1} \begin{bmatrix} B_{2g}'X_{gg}A_g + D_{12}'C_{1g} & B_{2g}'X_{gd}A_d + B_{2g}'X_{gg}B_{1gr}C_{d1} \\ D_{12}'D_{11gr}C_{d1} \end{bmatrix} = [F_{2g} \quad F_{2d}] \quad (18) \quad 305$$

and hence  $F_{2g}$  and  $F_{2d}$  form partitions of  $F_2$ . Now, partition Eq. (9) to obtain 308



$$\begin{aligned} \begin{bmatrix} X_{gg} & X_{gd} \\ X'_{gd} & X_{dd} \end{bmatrix} &= \begin{bmatrix} A'_g & 0 \\ C'_{d1}B'_{1gr} & A'_d \end{bmatrix} \begin{bmatrix} X_{gg} & X_{gd} \\ X'_{gd} & X_{dd} \end{bmatrix} \begin{bmatrix} A_g & B_{1gr}C_{d1} \\ 0 & A_d \end{bmatrix} \\ &- \begin{bmatrix} F'_{2g} \\ F'_{2d} \end{bmatrix} \bar{R} \begin{bmatrix} F_{2g} & F_{2d} \end{bmatrix} + \begin{bmatrix} C'_{1g} \\ C'_{d1}D'_{11gr} \end{bmatrix} \\ &\times \begin{bmatrix} C_{1g} & D_{11gr}C_{d1} \end{bmatrix} \end{aligned} \quad (19)$$

Equation (15) is easily checked, and so Eqs. (13), (16), and (17) follow immediately by considering, respectively, the top left, the top right, and the bottom right partitions of Eq. (19). Now, note that

$$A_c = \begin{bmatrix} A_{cg} & \star \\ 0 & A_d \end{bmatrix}$$

in which  $A_d$  is stable. It now follows from assumption (A1) that  $X_{gg}$  is stabilizing if and only if  $X$  is stabilizing.  $\square$

Note that  $F_{2g}$  and  $\bar{R}$  are not functions of  $X_{gd}$  or  $X_{dd}$ , and so Eq. (13) may be solved independently by Eqs. (16) and (17). Since Eq. (16) depends on the solution of Eq. (13), it can be solved next. Finally, Eq. (17) depends on both Eqs. (13) and (16) and so it is necessarily solved last. The following result provides a fast algorithm for solving Eq. (16).

Lemma 4.2 (efficient solution of the Stein equation). Consider the discrete Stein equation

$$X_{gd} = SC_{d1} + A'_{cg}X_{gd}A_d \quad (20)$$

with  $A_{cg}$  stable. Partitioning  $X_{gd} = [X_{gp} \ X_{gr}]$  compatibly with

$$A_d = \begin{bmatrix} A_p & B_pC_r \\ 0 & A_r \end{bmatrix}$$

gives

$$X_{gp} = [S \ A'_{cg}S \ A'^2_{cg}S \ \dots \ A'^{N-1}_{cg}S] \quad (21)$$

$$X_{gr} = A'^N_{cg}SC_r + A'_{cg}X_{gr}A_r \quad (22)$$

Proof. Partitioning Eq. (20) leads to

$$X_{gp} = SC_p + A'_{cg}X_{gp}A_p \quad (23)$$

$$X_{gr} = A'_{cg}X_{gp}B_pC_r + A'_{cg}X_{gr}A_r \quad (24)$$

If we substitute Eq. (23) into itself  $M$  times we obtain

$$X_{gp} = A'^{M+1}_{cg}X_{gp}A_p^{M+1} + \sum_{k=0}^M A'^k_{cg}SC_pA_p^k$$

Since  $A_{cg}$  and  $A_p$  are stable, we may allow  $M \rightarrow \infty$  and hence write

$$X_{gp} = \sum_{k=0}^{\infty} A'^k_{cg}SC_pA_p^k$$

However, since  $A_p^N = 0$  we may truncate the infinite sum to give

$$X_{gp} = \sum_{k=0}^{N-1} A'^k_{cg}SC_pA_p^k \quad (25)$$

The effect of postmultiplying by  $A_p^k$  is to shift the columns of the preceding matrix right by  $kl_r$ , and so  $C_pA_p^k = [0_{l_r \times kl_r} \ I_{l_r} \ 0_{l_r \times (N-1-k)l_r}]$ . Substituting this into Eq. (25) leads to Eq. (21). Now, substituting Eq. (21) into Eq. (24) leads to Eq. (22).  $\square$

The following is obtained by substituting Eqs. (21) and (22) into the definitions for the controller gains  $F_2$  and  $F_0$ .

Corollary 4.3 (efficient computation of full-information controller gains). The matrix  $F_2$  may be partitioned (compatibly with  $A$ ) as  $F_2 = [F_{2g} \ F_{2p} \ F_{2r}]$  in which  $F_{2g}$  is given by Eq. (14), and

$$\begin{aligned} F_{2p} &= -\bar{R}^{-1} [B'_{2g}X_{gg}B_{1gr} \\ &+ D'_{12}D_{11gr} \ B'_{2g}S \ B'_{2g}A'_{cg}S \ \dots \ B'_{2g}A'^{N-2}_{cg}S] \end{aligned} \quad (26)$$

$$F_{2r} = -\bar{R}^{-1} (B'_{2g}A'^{N-1}_{cg}SC_r + B'_{2g}X_{gr}A_r) \quad (27)$$

If we partition  $F_0 = [F_{0r} \ F_{0w}]$ , then

$$F_{0r} = -\bar{R}^{-1} (B'_{2g}X_{gr}B_r + B'_{2g}A'^{N-1}_{cg}SD_r) \quad (28)$$

$$F_{0w} = -\bar{R}^{-1} (B'_{2g}X_{gg}B_{1gw} + D'_{12}D_{11gw}) \quad (29)$$

Corollary 4.4. As  $N \rightarrow \infty$  the control becomes independent of the choice of  $W_r$ .

Proof. Since  $A_r$  and  $A_{cg}$  are asymptotically stable, it follows from standard results that Eq. (22) has a unique solution. In the limit as  $N \rightarrow \infty$ , Eq. (22) implies that  $X_{gr} = A'^N_{cg}X_{gr}A_r$  and so in the limit  $X_{gr} = 0$ . Direct substitution into Eqs. (27) and (28), while taking the limit as  $N \rightarrow \infty$ , leads to

$$F_{2r} = 0 \text{ and } F_{0r} = 0, \quad \forall A_r, B_r, C_r, D_r$$

and so the control signal is independent of  $W_r$ .

Remark 4.5. If  $x_g$  and  $x_r$  are the states of  $G$  and  $W_r$ , respectively, then the optimal control is given by

$$\begin{aligned} u(k)^* &= F_{2g}x_g(k) \\ &+ \underbrace{F_{2r}x_r(k) + F_{0r}\eta(k) + F_{0w}w(k) + \sum_{j=0}^{N-1} F_{2p,j}r(k-N+j)}_{\text{Feedforward}} \end{aligned}$$

with

$$F_{2p,0} = -\bar{R}^{-1} (B'_{2g}X_{gg}B_{1gr} + D'_{12}D_{11gr})$$

$$F_{2p,j} = -\bar{R}^{-1} B'_{2g}A'^j_{cg}S, \quad 1 \leq j \leq N-1$$

Remark 4.6. The feedback gain  $F_{2g}$  is precisely that which would be obtained if one were to search for a full-information controller that minimized  $\|T_{w \rightarrow z}\|$ , with  $W_r$  and  $\Phi$  removed from the problem description. The choice of feedback control is therefore independent of the preview length.

Remark 4.7. The full-information controller that minimizes  $\|T_{v \rightarrow z}\|_2$  also minimizes  $\|T_{\eta \rightarrow z}\|_2$  and  $\|T_{w \rightarrow z}\|_2$ . This type of relationship is true for any partition of the exogenous disturbance signal in an  $\mathcal{H}_2$  full-information generalized regulator problem, and it is not a particular feature of the preview control problem. To see this, note that the two minimization problems

$$\min_{K_{FI}} \|T_{\eta \rightarrow z}\|_2 \quad (30)$$

$$\min_{K_{FI}} \|T_{w \rightarrow z}\|_2 \quad (31)$$

are related by the choice of  $B_1$  and  $D_{11}$ , and that computation of the controller gain  $F_2$  is independent of these matrices. The feedforward control gains  $F_{0r}$  and  $F_{0w}$  can be chosen independently, and so it is possible to simultaneously minimize  $\|T_{\eta \rightarrow z}\|_2$  and  $\|T_{w \rightarrow z}\|_2$ . Since  $\|T_{v \rightarrow z}\|_2^2 = \|T_{\eta \rightarrow z}\|_2^2 + \|T_{w \rightarrow z}\|_2^2$ , a controller satisfying Eqs. (30) and (31) also minimizes  $\|T_{v \rightarrow z}\|_2$ .

## 5 Output-Feedback Solution

5.1 Standard Theory. We now consider a discrete-time, linear, time-invariant system  $P$  of the form

$$P = \begin{bmatrix} n & l & m \\ \leftrightarrow & \leftrightarrow & \leftrightarrow \\ \begin{matrix} n \\ p \\ q \end{matrix} \downarrow & \begin{bmatrix} A & B_1 & B_2 \\ C_1 & D_{11} & D_{12} \\ C_2 & D_{21} & 0 \end{bmatrix} \end{bmatrix}$$

396

397 which satisfies (A1)–(A3) as well as

398 (A4)  $(A, C_2)$  is detectable.

399 (A5)  $D_{21}D'_{21} > 0$ .

400 (A6)  $\text{rank} \begin{bmatrix} A - e^{j\theta} I & B_1 \\ C_2 & D_{21} \end{bmatrix} = n + q, \quad \forall \theta \in (-\pi, \pi]$ .

401 We wish to compute an internally stabilizing  $K$  that minimizes

402  $\|F_l(P, K)\|_2$ . Define

$$403 \quad \bar{S} = D_{21}D'_{21} + C_2Y C'_2, \quad L_2 = -(A Y C'_2 + B_1 D'_{21})\bar{S}^{-1}$$

404 If (A4)–(A6) are satisfied, it is shown in Ref. [17] that there exists

405 a  $Y$  that solves

$$406 \quad Y = A Y A' - L_2 \bar{S} L'_2 + B_1 B'_1 \quad (32)$$

407 such that

$$408 \quad Y \geq 0$$

409  $A + L_2 C_2$  is asymptotically stable.

410 If we define

$$411 \quad L_0 = (F_2 Y C'_2 + F_0 D'_{21})\bar{S}^{-1}$$

412 then, according to Ref. [17], the  $\mathcal{H}_2$ -optimal output-feedback con-  
413 troller is given by

$$414 \quad K = \begin{bmatrix} A_K & B_K \\ C_K & D_K \end{bmatrix} \quad (33)$$

$$415 \quad A_K = A + B_2 F_2 + L_2 C_2 - B_2 L_0 C_2 \quad (34)$$

$$416 \quad B_K = -(L_2 - B_2 L_0) \quad (35)$$

$$417 \quad C_K = F_2 - L_0 C_2 \quad (36)$$

$$418 \quad D_K = L_0 \quad (37)$$

419 The  $\mathcal{H}_2$ -norm of the resulting closed-loop system is given by

$$420 \quad \|F_l(P, K)\|_2^2 = \|F_l(P_F, K_F)\|_2^2 + \text{Tr}\{\bar{R}((L_0 D_{21} - F_0)(L_0 D_{21} - F_0)' \\ 421 \quad + (L_0 C_2 - F_2)Y(L_0 C_2 - F_2)')\}$$

## 422 5.2 Efficient Computation of Output-Feedback Controller.

423 In this section we aim to find a computationally efficient solution  
424 to the DARE in Eq. (32), given that  $P$  has the structure described  
425 in Eq. (4). The results of this section do not depend on the internal  
426 structure of  $A_p$ ,  $B_p$ , and  $C_p$  (though we do require that  $A_p$  is  
427 stable).

428 Lemma 5.1. The stabilizing non-negative solution to Eq. (32)  
429 may be computed using

$$Y = \begin{bmatrix} n_g & n_l + n_r \\ \leftrightarrow & \leftrightarrow \\ \begin{matrix} n_g \\ n_l + n_r \end{matrix} \downarrow & \begin{bmatrix} Y_g & 0 \\ 0 & 0 \end{bmatrix} \end{bmatrix} \quad \text{alignment problem}$$

430

431 where  $Y_g$  is the unique stabilizing and non-negative solution to

$$432 \quad Y_g = A_g Y_g A'_g - L_{2g} \bar{S}_g L'_{2g} + B'_{1gw} B_{1gw} \quad (38)$$

433 with

$$\bar{S}_g = D_{21gw} D'_{21gw} + C_{2g} Y_g C'_{2g}, \quad L_{2g} = -(A_g Y_g C'_{2g} + B_{1gw} D'_{21gw})\bar{S}_g^{-1} \quad 434$$

Proof. Note that (A4)–(A6) imply 435

(A4g)  $(A_g, C_{2g})$  is detectable. 436

(A5g)  $D_{21gw} D'_{21gw} > 0$ . 437

(A6g)  $\text{rank} \begin{bmatrix} A_g - e^{j\theta} I & B_{1gw} \\ C_{2g} & D_{21gw} \end{bmatrix} = n_g + q_g, \quad \forall \theta \in (-\pi, \pi]$ . 438

It then follows that (A4)–(A6) ensure the existence of a stabi- 439  
lizing non-negative solution to Eq. (38). Let  $Y_g$  be a stabilizing 440  
and non-negative solution to Eq. (38). We will now show that  $Y$  441  
 $= \begin{bmatrix} Y_g & 0 \\ 0 & 0 \end{bmatrix}$  is a stabilizing non-negative solution to Eq. (32). 442

It easily checked that the following hold, if  $Y = \begin{bmatrix} Y_g & 0 \\ 0 & 0 \end{bmatrix}$ : 443

$$\bar{S} = \begin{bmatrix} \bar{S}_g & 0 \\ 0 & D_r D'_r \end{bmatrix} \quad 444$$

$$L_2 = \begin{bmatrix} L_{2g} & 0 \\ 0 & -B_d D_r^{-1} \end{bmatrix} \quad 445$$

$$B_1 B'_1 = \begin{bmatrix} B_{1gw} B'_{1gw} & 0 \\ 0 & B_d B'_d \end{bmatrix} \quad 446$$

$$A Y A' = \begin{bmatrix} A_g Y_g A'_g & 0 \\ 0 & 0 \end{bmatrix} \quad (39) \quad 447$$

where the invertibility of  $D_r$  is guaranteed by assumption (A5), 448  
together with the fact that  $W_r$  is square. It then follows that: 449

$$A Y A' - L_2 \bar{S} L'_2 + B_1 B'_1 = \begin{bmatrix} A_g Y_g A'_g - L_{2g} \bar{S}_g L'_{2g} + B_{1gw} B'_{1gw} & 0 \\ 0 & 0 \end{bmatrix} \quad 450$$

$$= \begin{bmatrix} Y_g & 0 \\ 0 & 0 \end{bmatrix} = Y \quad 451$$

Therefore, if  $Y_g$  solves Eq. (38), then  $Y = \begin{bmatrix} Y_g & 0 \\ 0 & 0 \end{bmatrix}$  solves Eq. (32). 452  
We now need to check that  $Y$  is stabilizing. Note that 453

$$A + L_2 C_2 = \begin{bmatrix} A_g + L_{2g} C_{2g} & \star \\ 0 & A_d - B_d D_r^{-1} C_{d2} \end{bmatrix} \quad 454$$

The matrix  $A_d - B_d D_r^{-1} C_{d2}$  is stable because 455

$$A_d - B_d D_r^{-1} C_{d2} = \begin{bmatrix} A_p & 0 \\ 0 & A_r - B_r D_r^{-1} C_r \end{bmatrix} \quad (40) \quad 456$$

in which  $A_p$  is stable by definition and  $A_r - B_r D_r^{-1} C_r$  is stable be- 457  
cause  $W_r$  is assumed to be outer. Since  $Y_g$  is stabilizing, we know 458  
that  $A_g + L_{2g} C_{2g}$  is stable, and hence that  $A + L_2 C_2$  is stable, as 459  
required. 460

**5.3 Efficient Implementation.** We now have a complete 461  
method for efficiently computing the output-feedback preview 462  
controller; however, in its present form, this controller has the 463  
same order as the generalized plant. In general, a controller of this 464  
order cannot be implemented. Fortunately, the high-order part of 465  
the controller is a FIR filter (illustrated in Fig. 4) for which effi- 466  
cient implementations exist. 467

This controller structure is proven in the following lemma. 468

Lemma 5.2. The optimal controller described in Eq. (33) for the 469  
plant in Eq. (4) can be written in the form 470

$$K = \begin{bmatrix} A_K & B_K \\ C_K & D_K \end{bmatrix} = \begin{bmatrix} A_{Kgg} & A_{Kgp} & A_{Kgr} & B_{Kgy} & B_{Kgr} \\ 0 & A_p & 0 & 0 & B_p \\ 0 & 0 & A_r - B_r D_r^{-1} C_r & 0 & B_r D_r^{-1} C_r \\ C_{Kg} & C_{Kp} & C_{Kr} & L_{0y} & F_{0r} D_r^{-1} \end{bmatrix} \quad (41) \quad 471$$

where  $A_{Kgg} \in \mathbb{R}^{n_g \times n_g}$  and  $B_{Kgg} \in \mathbb{R}^{n_g \times l_w}$  and 472

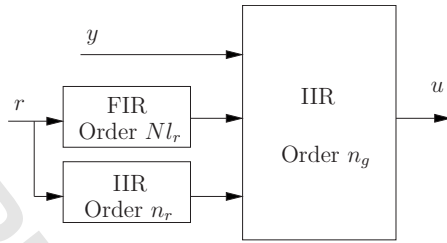


**Fig. 4** Structure of the  $\mathcal{H}_2$ -optimal preview controller. The signal  $u$  is the control, the measurement is  $y$ , and  $r$  is the future value of the previewable disturbance. The preview length is  $N$ ,  $l_r$  is the dimension of  $r$ ,  $n_r$  is the order of  $W_r$ , and  $n_g$  is the order of  $G$ .

$$L_{0y} = (F_{2g}Y_gC'_{2g} + F_{0w}D'_{21gw})\bar{S}_g^{-1}$$

$$A_{Kgg} = A_g + B_{2g}F_{2g} + L_{2g}C_{2g} - B_{2g}L_{0y}C_{2g}$$

$$A_{Kgp} = B_{1gr}C_p + B_{2g}F_{2p} + L_{2g}D_{21gr}C_p - B_{2g}L_{0y}D_{21gr}C_p$$

$$A_{Kgr} = B_{2g}F_{2r} - B_{2g}F_{0r}D_r^{-1}C_r$$

$$B_{Kgy} = -(L_{2g} - B_{2g}L_{0g})$$

$$B_{Kgr} = B_{2g}F_{0r}D_r^{-1}$$

$$C_{Kg} = F_{2g} - L_{0y}C_{2g}$$

$$C_{Kp} = F_{2p} - L_{0y}D_{21gr}C_p$$

$$C_{Kr} = F_{2r} - F_{0r}D_r^{-1}C_r$$

*Proof.* The realization given in Eq. (41) follows from Eq. (33), together with Eqs. (39) and (40), and  $L_0 = [L_{0y} \ F_{0r}D_r^{-1}]$ .  $\square$

This then leads to the low-order implementation

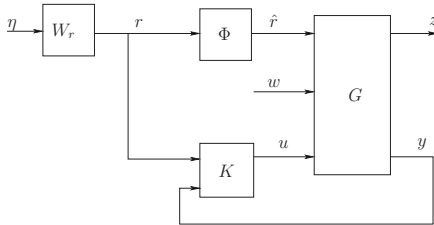
$$\bar{K} \stackrel{s}{=} \begin{bmatrix} A_{Kgg} & A_{Kgr} & B_{Kgy} & A_{Kgp} & B_{Kgr} \\ 0 & A_r - B_rD_r^{-1}C_r & 0 & 0 & B_rD_r^{-1} \\ C_{Kg} & C_{Kr} & L_{0y} & C_{Kp} & F_{0r}D_r^{-1} \end{bmatrix} \quad (42)$$

where the optimal control is given by

$$u^* = \bar{K} \begin{bmatrix} y \\ \bar{r} \end{bmatrix}$$

$$\bar{r}(k) = \begin{bmatrix} r(k-N) \\ \vdots \\ r(k) \end{bmatrix}$$

**Corollary 5.3.** The output-feedback controller that minimizes  $\|T_{v \rightarrow z}\|_2$ , also minimizes  $\|T_{\eta \rightarrow z}\|_2$  and  $\|T_{w \rightarrow z}\|_2$ .



*Proof.* The controller may be decomposed into feedback and feedforward components  $K_{fb}$  and  $K_{ff}$ , so that

$$u^* = K_{fb}y + K_{ff}r$$

with  $K_{fb}$  given by

$$K_{fb} \stackrel{s}{=} \begin{bmatrix} A_{Kgg} & B_{Kgy} \\ C_{Kg} & L_{0y} \end{bmatrix}$$

The transfer function  $T_{w \rightarrow z}$  is determined by  $K_{fb}$  and  $P$ , and it is easily checked that  $K_{fb}$  is precisely the controller, which is obtained by minimizing  $\|T_{w \rightarrow z}\|_2$  alone.

It is well known that the  $\mathcal{H}_2$ -optimal controller has an observer structure. If  $w=0$ , then the observer will contain an exact copy of the states of  $G$  and  $W_r$  (once initial transients have decayed). Therefore, the closed-loop transfer function  $T_{r \rightarrow z}$  will be precisely the same as that resulting from the application of the full-information controller  $K_{FI}$  to the plant  $P_{FI}$ . Remark 4.7 implies that the value of  $\|T_{r \rightarrow z}\|_2$  achieved by this controller is indeed minimal.  $\square$

Unlike the full-information case, this result is not a general property of any partition of the exogenous disturbance signal, instead it results from the particular structure considered here. The result is useful because it leads us to the conclusion that the choice of  $W_r$  does not alter the resulting  $T_{w \rightarrow z}$ , and so  $W_r$  tunes only the response to the previewable signal.

## 6 Reduction in $\mathcal{H}_2$ -Norm Due to Preview

The purpose of this section is to derive an efficient means of computing the minimum achievable closed-loop  $\mathcal{H}_2$ -norm for a given preview length. In so doing, we provide tools to answer the questions:

- What is the preview length required to achieve a given performance specification?
- What is the maximum possible reduction in the closed-loop  $\mathcal{H}_2$ -norm through preview?
- If a large amount of preview is available, how much should be used?

For the purposes of computing the minimum achievable  $\mathcal{H}_2$ -norm, we may assume  $W_r=I$  without loss of generality. The transformation that enables us to make this assumption is illustrated in Fig. 5. The design problem involving  $\hat{K}$  and  $\hat{G}$  is clearly a problem of the class of Fig. 1, but without a prefilter. The achievable  $\mathcal{H}_2$ -norm will be the same in either case, and in this section we will work with the simpler problem setup, where it is assumed that  $W_r$  has been absorbed into  $\hat{G}$  and  $\hat{K}$ . This transformation is not used in the preceding sections because it obscures the impact of  $W_r$  on the control signal, and because we would be required to perform further manipulations in order to remove the additional controller states resulting from the extra copy of  $W_r$ .

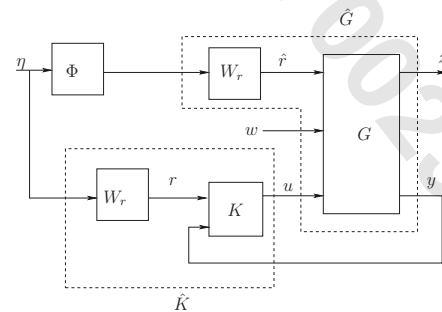


**Fig. 5** Two equivalent representations of the previewable disturbance rejection problem. These representations are equivalent in the sense that the transfer functions from  $\eta$  and  $w$  to  $z$  and  $y$  are identical. Recall that  $\Phi = \mathcal{Z}^{-N}I$ , which commutes with  $W_r$  under multiplication.

It is easy to check that the results of the previous sections carry over for  $W_r = I$ . All that is required is to remove the gains associated with the states of  $W_r$ . We note again that

$$\|T_{[r'w'] \rightarrow z}\|_2^2 = \|T_{w \rightarrow z}\|_2^2 + \|T_{r \rightarrow z}\|_2^2 \quad (43)$$

As observed in Corollary 5.3, the optimal preview controller minimizes  $\|T_{w \rightarrow z}\|_2$ . Since  $X_{gg}$  and  $Y_g$  are the solutions to the DAREs associated with the problem of minimizing  $\|T_{w \rightarrow z}\|_2$ , we may use the results in Secs. 4.1 and 5.1 to write

$$\gamma_{wc}^2 = \text{Tr}\{(D_{11gw} + D_{12}F_{0w})'(D_{11gw} + D_{12}F_{0w}) + (B_{1gw} + B_{2g}F_{0w})'X_{gg}(B_{1gw} + B_{2g}F_{0w})\}$$

$$\gamma_{wf}^2 = \text{Tr}\{\bar{R}((L_{0y}D_{21gw} - F_{0w})(L_{0y}D_{21gw} - F_{0w})' + (L_{0y}C_{2g} - F_{2g})Y_{gg}(L_{0y}C_{2g} - F_{2g})')\}$$

$$\|T_{w \rightarrow z}\|_2^2 = \gamma_{wc}^2 + \gamma_{wf}^2$$

which are independent of the preview length.

We now turn our attention to the evaluation of  $\|T_{r \rightarrow z}\|_2$ . Since the signal  $r$  is "known" to the controller, it does not introduce an estimation error. As a result the output-feedback controller achieves exactly the same transfer function  $T_{r \rightarrow z}$  as the full-information controller  $K_{FI}$ . Thus

$$T_{r \rightarrow z} = \begin{bmatrix} A + B_2F_2 & B_{2g}F_{0r} \\ C_1 + D_{12}F_2 & D_{12}F_{0r} \end{bmatrix}$$

Note that  $X$  satisfies

$$(A + B_2F_2)'X(A + B_2F_2) + (C_1 + D_{12}F_2)'(C_1 + D_{12}F_2)$$

and so using Eq. (3) we may write

$$\|T_{r \rightarrow z}\|_2^2 = \text{Tr}\left\{(D_{12}F_{0r})'D_{12}F_{0r} + \begin{bmatrix} B_{2g}F_{0r} \\ B_p \end{bmatrix}' \begin{bmatrix} X_{gg} & X_{gp} \\ X'_{gp} & X_{pp} \end{bmatrix} \times \begin{bmatrix} B_{2g}F_{0r} \\ B_p \end{bmatrix}\right\}$$

where  $F_{0r} = -\bar{R}^{-1}B_{2g}'X_{gg}B_p$ . The above expression may be simplified to

$$\|T_{r \rightarrow z}\|_2^2 = \text{Tr}\{B_p'X_{pp}B_p - F_{0r}'\bar{R}F_{0r}\} \quad (44)$$

Our next task is to find an efficient method for computing  $B_p'X_{pp}B_p$ . Using the  $W_r = I$  version of Eq. (17), we can write

$$X_{pp} = A_p'X_{pp}A_p + \hat{Q} - F_{2p}'\bar{R}F_{2p}$$

in which

$$\hat{Q} = C_p'B_{1gr}'X_{gg}B_{1gr}C_p + A_p'X_{gp}'B_{1gr}C_p + C_p'B_{1gr}'X_{gp}A_p + C_p'D_{11gr}'D_{11gr}C_p$$

Substituting this into itself leads to

$$X_{pp} = \sum_{j=0}^{N-1} A_p^j(\hat{Q} - F_{2p}'\bar{R}F_{2p})A_p^j$$

Note that postmultiplying by  $A_p^k B_p$  has the effect of selecting individual block columns of the preceding matrix that  $C_p A_p^k B_p = 0$ ,  $\forall k \neq N-1$ , and that  $A_p^N = 0$ . This means that

$$B_p'X_{pp}B_p = B_{1gr}'X_{gg}B_{1gr} + D_{11gr}'D_{11gr} - F_{2p0}'\bar{R}F_{2p0} - \sum_{j=0}^{N-2} S'A_{cg}^j B_{2g}\bar{R}^{-1}B_{2g}'A_{cg}^j S$$

where  $F_{2p0}$  is the leftmost block column of  $F_{2p}$  and is given by

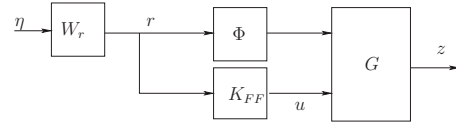


Fig. 6 A feedforward controller design problem. The notation follows that of Fig. 1.

$$F_{2p0} = -\bar{R}^{-1}(B_{2g}'X_{gg}B_{1gr} + D_{12}'D_{11gr}) \quad (45)$$

Combining this with Eq. (44) and using Eq. (21), leads to

$$\|T_{r \rightarrow z}\|_2^2 = \text{Tr}\left\{\underbrace{B_{1gr}'X_{gg}B_{1gr} + D_{11gr}'D_{11gr} - F_{2p0}'\bar{R}F_{2p0}}_{\text{Zero preview}} - \underbrace{\sum_{j=0}^{N-1} S'A_{cg}^j B_{2g}\bar{R}^{-1}B_{2g}'A_{cg}^j S}_{\text{Preview reduction}}\right\} \quad (46)$$

In order to judge how much preview to use, we need to know the value of the maximum possible improvement due to preview action. Suppose the matrix  $\Gamma$  satisfies

$$\Gamma = A_{cg}\Gamma A_{cg}' + B_{2g}\bar{R}^{-1}B_{2g}'$$

By repeatedly substituting for  $\Gamma$  in the above equation, and noting that  $A_{cg}$  is stable, we can write

$$\Gamma = \sum_{j=0}^{\infty} A_{cg}^j B_{2g}\bar{R}^{-1}B_{2g}'A_{cg}^j$$

Comparing this to Eq. (46), it follows that the maximum reduction in  $\|T_{r \rightarrow z}\|_2^2$  due to preview is given by

$$\text{Tr}\{S'\Gamma S\}$$

and evaluating this limit only requires the solution of an  $n_g$ -dimensional Lyapunov equation (in addition to the  $n_g$ -dimensional DARE required to evaluate  $S$ ). The following quantity provides a useful measure of the fraction of the maximum norm reduction that has been achieved:

$$\gamma_{\%,imp} = 100 \times \text{Tr}\left\{\left(\sum_{j=0}^{N-1} S'A_{cg}^j B_{2g}\bar{R}^{-1}B_{2g}'A_{cg}^j S\right) / \text{Tr}\{S'\Gamma S\}\right\} \quad (47)$$

This can be used to determine how much preview to use; for example, one might continue adding preview points until  $\gamma_{\%,imp} > 95\%$ .

## 7 Computation of a Preview Feedforward Controller

In this section we consider the problem of designing a feedforward controller. Such a problem may arise if there is no feedback signal, or if we wish to use a preview precompensator to enhance an existing feedback controller.

Potentially, one could formulate a feedforward problem by removing the measurement signal  $y$  from the configuration in Fig. 1. However, if we recall that

$$\|T_{[\eta'w'] \rightarrow z}\|_2^2 = \|T_{w \rightarrow z}\|_2^2 + \|T_{\eta \rightarrow z}\|_2^2$$

and that a feedforward controller does not alter  $T_{w \rightarrow z}$ , then it follows that  $\|T_{[\eta'w'] \rightarrow z}\|_2$  is minimized by choosing the feedforward controller, which minimizes  $\|T_{\eta \rightarrow z}\|_2$ . Given these observations, we may neglect the influence of  $w$  in the design process.

The problem considered in this section is illustrated in Fig. 6.



616 Such a configuration is apparently a special case of Fig. 1, and so  
617 it is tempting to try to tackle this problem by using the above  
618 general theory with  $y$  set to zero (by setting  $D_{21gw}$ ,  $D_{21gr}$ ,  $C_{2g}$ , and  
619  $D_{22g}$  to zero) and with  $w$  removed. Unfortunately, such an ap-  
620 proach does not succeed because assumption (A5) is violated. We  
621 will now derive a solution to this problem.

622 By modifying Eq. (4), it follows that the appropriate general-  
623 ized plant is given by

624 
$$P_{FF} = \begin{array}{c|cc|cc} \begin{array}{c} A_g \quad B_{1gr}C_{d1} \quad 0 \\ 0 \quad A_d \quad B_d \\ C_{1g} \quad D_{11gr}C_{d1} \quad 0 \\ 0 \quad C_{d2} \quad D_r \end{array} & \begin{array}{c} B_{2g} \\ 0 \\ D_{12} \\ 0 \end{array} \\ \hline \end{array} \quad (48)$$

625 
$$= \begin{array}{c|cc} \begin{array}{c} A \quad B_1 \quad B_2 \\ C_1 \quad D_{11} \quad D_{12} \\ C_2 \quad D_{21} \quad 0 \end{array} \\ \hline \end{array} \quad (49)$$

626 It is easily checked that the associated full-information control  
627 is obtained by removing the gain associated with  $w$ , and so  $K_{FI}$   
628  $= [F_{2g} \ F_{2p} \ F_{2r} \ F_{0r}]$ , where the gains may be computed using  
629 Eqs. (14) and (26)–(28). To arrive at this result, one only needs to  
630 retrace the derivations of Sec. 4, with  $B_{1gw}$  and  $D_{11gw}$  set to zero.  
631 Next, we give a result concerning the solution to the estimation  
632 DARE.

633 Lemma 7.1. *If  $A_g$  is stable and  $W_r$  is outer, then the version of*  
634 *the DARE in Eq. (32) associated with Eq. (48) has a stabilizing*  
635 *solution  $Y=0$ .*

636 *Proof.* First, note that if  $Y=0$ , then

637 
$$L_2 = - \begin{bmatrix} 0 \\ B_d D_r^{-1} \end{bmatrix}$$

653  
654

$$\bar{K}_{FF} = \begin{array}{c|cc|cc} \begin{array}{c} A_g + B_{2g}F_{2g} \quad B_{2g}F_{2r} - B_{2g}F_{0r}D_r^{-1}C_r \\ 0 \quad A_r - B_rD_r^{-1}C_r \\ F_{2g} \quad F_{2r} - F_{0r}D_r^{-1}C_r \end{array} & \begin{array}{c} B_{1gr}C_p + B_{2g}F_{2p} \quad B_{2g}F_{0r}D_r^{-1}C_r \\ 0 \quad B_rD_r^{-1} \\ F_{2p} \quad F_{0r}D_r^{-1} \end{array} \\ \hline \end{array}$$

655  
656  
657  
658

659 such that the optimal control is given by

660 
$$u^* = \bar{K}_{FF}\bar{r}$$

661 in which

662 
$$\bar{r}(k) = \begin{bmatrix} r(k-N) \\ \vdots \\ r(k) \end{bmatrix}$$

## 663 8 Summary of Results

664 Our purpose here is to provide a summary of the major features  
665 of  $\mathcal{H}_2$  preview controllers, which will hopefully be of assistance  
666 to control system designers. While some of these results are  
667 known within the control systems community, they are spread  
668 over many publications spanning three decades.

### 669 8.1 Generic Controller Features

670 8.1.1 *Riccati Equation Solutions.* Synthesizing the output-  
671 feedback controller requires the solution of a full-information Ricci-  
672 cati equation and a Kalman filtering equation [16,17]. Although  
673 these equations appear to be of high order, the full-information  
674 control problem only requires the solution of the  $n_g$ -dimensional  
675 Riccati equation (13), while the estimation problem requires the

638 
$$\bar{S} = D_r D_r'$$
 638

639 from which it can be checked that  $Y=0$  solves Eq. (32). This  
640 solution is stabilizing because 640

641 
$$A + L_2 C_2 = \begin{bmatrix} A_g & B_{1gr}C_{d1} \\ 0 & A_d - B_d D_r^{-1} C_{d2} \end{bmatrix}$$
 641

is stable since  $A_g$  is stable and  $W_r$  is outer (see Eq. (40)). □ 642

If we also note that 643

644 
$$L_0 = F_{0r} D_r^{-1}$$
 644

645 with  $F_{0r}$  defined in Eq. (28), then we can use Eq. (33) to obtain  
646 the following  $\mathcal{H}_2$ -optimal controller 646

647 
$$K_{FF} = \begin{bmatrix} A_K & B_K \\ C_K & D_K \end{bmatrix}$$
 647

648 
$$A_K = \begin{bmatrix} A_g + B_{2g}F_{2g} & B_{1gr}C_p + B_{2g}F_{2p} & B_{2g}F_{2r} - B_{2g}F_{0r}D_r^{-1}C_r \\ 0 & A_p & 0 \\ 0 & 0 & A_r - B_rD_r^{-1}C_r \end{bmatrix}$$
 648

649 
$$B_K = \begin{bmatrix} B_{2g}F_{0r}D_r^{-1} \\ B_p \\ B_rD_r^{-1} \end{bmatrix}$$
 649

650 
$$C_K = [F_{2g} \ F_{2p} \ F_{2r} - F_{0r}D_r^{-1}C_r]$$
 650

651 
$$D_K = F_{0r}D_r^{-1}$$
 651

which has the low-order representation 652

676 solution of the  $n_g$ -dimensional Riccati equation (38). The bulk of  
677 the full-information Riccati equation can be evaluated using the  
678 linear equations (16) and (17). The DARE in Eq. (13) is precisely  
679 that which would be obtained if one were to search for a full-  
680 information controller, which minimized  $\|T_{w \rightarrow z}\|$ . 680

681 It is important to note that  $F_{2g}$  and  $\bar{R}$  are not functions of  $X_{gd}$  or  
682  $X_{dd}$ , and so Eq. (13) may be solved independently of Eqs. (16) and  
683 (17). However, Eq. (16) depends on the solution of Eq. (13), and  
684 Eq. (17) depends on both Eqs. (13) and (16). Lemma 4.2 provides  
685 a fast algorithm for solving Eq. (16). 685

686 8.1.2 *Full-Information Control Structure.* The full-information  
687 control signal has the form 687

688 
$$u(k)^* = \hat{u}(k) + \sum_{j=0}^{N-1} F_{2p,j} r(k-N+j)$$
 688

689 in which  $\hat{u}(k)$  is a linear function of the states of  $G$  and  $W_r$ , and of  
690 the signals  $\eta$  and  $w$ ; the  $F_{2p,j}$  are sometimes referred to as the  
691 “preview gains.” Further insight into the structure and role of the  
692 control signal components can be found in Remarks 4.5–4.7. 692

693 8.1.3 *The Preview Gains Decay to Zero as  $N \rightarrow \infty$ .* It was first  
694 noted in Ref. [6] that the magnitude of the preview gains ap-  
695 proaches zero as  $N$  approaches infinity; this follows from Eq. (26) 695

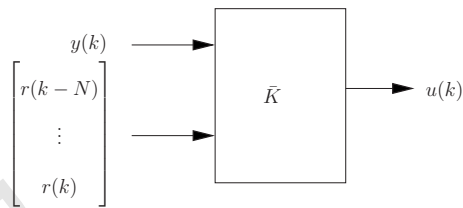


Fig. 7 The structure of the  $\mathcal{H}_2$ -optimal discrete-time preview controller. The signal  $u(k)$  is the control, the measurement is  $y(k)$ , and  $r(k)$  is the futuremost value of the previewable disturbance.

Font sizes too small with the diagram shrunk to this size. Could be increased via psfrag.

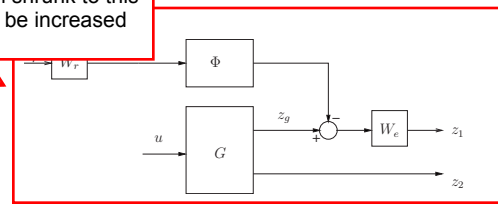


Fig. 8 A simple preview-tracking problem. The feedback signal is derived from the states of  $G$ ,  $W_r$ ,  $W_e$ , and  $\Phi$ , together with  $\eta$ . The signal  $u$  is the control,  $r$  is the previewed reference, and  $z=[z_1 z_2]'$  is the output to be minimized.

696 and  $\lim_{N \rightarrow \infty} A_{cg}^N = 0$ . As a consequence, far-distant preview infor-  
697 mation is relatively less important and the optimal infinite preview  
698 controller can be approximated to arbitrary accuracy using a finite  
699 preview length.

700 **8.1.4 The Controller Has FIR (Preview) and IIR Components.**  
701 Discrete-time preview controllers are composed of a high-order  
702 FIR preview component and low-order IIR components. This  
703 structure is illustrated in Fig. 5, and is also highlighted in the  
704 continuous-time case in Ref. [22]. A proof is provided for the  
705 discrete-time case in Sec. 5. If the controller is written in observer  
706 form, then the states of the FIR preview block and the order  $n_r$  IIR  
707 block are (perfect) reconstructions of the states of  $\Phi$  and  $W_r$ ,  
708 respectively. The state of the order  $n_g$  IIR block is an estimate for  
709 the state of  $G$ .

710 **8.1.5 The Controller is Essentially Low-Order.** A discrete-  
711 time FIR transfer function can be realized using a shift-register to  
712 update the state, and a gain array to compute the output. This  
713 representation leads to the low-order controller representation in  
714 Fig. 7, where  $\bar{K}$  is given by Eq. (42).

715 **8.1.6 The Optimal Control is Independent of  $W_r$  for Large  $N$ .**  
716 This phenomenon was first noticed in Ref. [6], with a proof pro-  
717 vided in Sec. 4. It is instructive to consider the influence of  $W_r$ ,  
718 from a stochastic perspective. Since  $\eta$  is assumed to be a realiza-  
719 tion of a white-noise process, then a dynamic  $W_r$  provides statis-  
720 tical information on future values of  $r$ . If, for example,  $W_r$  is  
721 low-pass, the  $r(k)$  becomes correlated and hence  $W_r$  introduces  
722 “statistical preview” beyond the preview horizon. We would  
723 therefore expect  $W_r$  to reduce the need for preview, and also that  
724 its influence on the control would decline as  $N$  tends to infinity.

725 **8.1.7 The Optimal  $\|T_{w \rightarrow z}\|_2$  Is Independent of  $W_r$ .** In contrast  
726 with the  $\mathcal{H}_\infty$  case [23], there is no conflict between the rejection of  
727  $w$  and the rejection of  $\eta$ ; a proof of this is provided in Sec. 5.

728 **8.1.8 Noisy Preview Signals Require a High-Order Controller.**  
729 One might consider an uncertain preview problem, where the con-  
730 troller has access only to a noise-corrupted version of the pre-  
731 viewed signal. In this scenario, the states of  $\Phi$  are not known, and  
732 must be estimated. The preview provides benefit both by reducing  
733 the full-information control cost and by reducing the estimation  
734 cost. Estimating the states of  $\Phi$  is a type of fixed-lag smoothing  
735 problem. Low-order implementations of fixed-lag smoothers are  
736 given in Ref. [24], but these implementations are not usable here  
737 because of the need for an estimate of all of the states of  $\Phi$ , rather  
738 than just the output of  $\Phi$ . The resulting controller is thus of the  
739 same order as the augmented plant. A controller for this problem  
740 may be synthesized by direct application of the results in Sec. 5.1.

741 **8.2 Design Insights.** This section provides a number of “rules  
742 of thumb” that the authors have found useful. For the purposes of  
743 illustration, we will consider the full-information preview-  
744 tracking problem described in Fig. 8, where  $G$  is given by

$$\hat{G} = \frac{1.26 \times 10^{-8} (Z+1)^3}{(Z-1)(Z^2 - 1.998Z + 0.998)} \quad 745$$

$$G = \begin{bmatrix} \hat{G} \\ 1 \end{bmatrix} \quad (50) \quad 746$$

The discrete transfer function  $\hat{G}$  was obtained by discretizing 747

$$\frac{101}{s(s^2 + 2s + 101)} \quad 748$$

using a sample time of 0.001 s. We search for a  $K$  that minimizes 749  
 $\|T_{\eta \rightarrow z}\|_{2,\infty}$ , or equivalently, the  $K$  that minimizes 750

$$\left\| \begin{bmatrix} W_e W_r T_{r \rightarrow e} \\ W_r T_{r \rightarrow u} \end{bmatrix} \right\|_{2,\infty} \quad (51) \quad 751$$

Clearly, this represents a tracking problem in which minimization 752  
of tracking errors must be balanced against excessive control re- 753  
quirements. The transfer functions  $W_r$  and  $W_e$  may be chosen to 754  
reflect, respectively, the expected frequency content of  $r$ , and the 755  
importance of achieving good tracking at a given frequency. We 756  
will now use this example to illustrate some general properties of 757  
 $\mathcal{H}_2$  preview-tracking controllers. 758

8.2.1 **Preview Improves Steady-State Tracking.** Figure 9 illus- 759  
trates the “nonresponsiveness” of the closed-loop system in the 760  
case of no reference weight and a low preview horizon. In the 761  
limiting case, where there is zero preview and no reference 762  
weighting, the controller does not have any information about the 763  
value of the reference at the next time step, and so it cannot make 764  
a decision about the direction in which to send the plant. There- 765  
fore, the tracking-error cost cannot be reduced, and so the optimal 766  
controller can only minimize the control cost, leading to a choice 767  
of  $u=0$ . 768

Alternatively, as  $N \rightarrow \infty$ , then the steady-state error tends toward 769  
zero (in the absence of disturbances or modeling errors). 770

8.2.2 **Reference Weighting Introduces Stochastic Preview.** The 771  
responses illustrated in Fig. 9 are unsatisfactory for preview hori- 772  
zons of less than  $N=200$ . When short preview horizons are man- 773  
dated, a low-pass  $W_r$  improves low-frequency tracking by biasing 774  
the controller optimization toward lower frequencies. It is worth 775  
noting, however, that care should be taken in choosing  $W_r$ . If, for 776  
example,  $W_r$  rolls off too quickly, the closed-loop will be poorly 777  
tuned for step inputs and can have an oscillatory response, and/or 778  
high-amplitude controls. This is because a low-pass  $W_r$  has the 779  
dual effect of penalizing low-frequency tracking errors, and also 780  
reducing the penalty on high frequency controls—see Eq. (51). 781  
The effect of a low-pass  $W_r$  is illustrated in Fig. 10. 782

8.2.3 **Tracking-Error Filtering.** Consider the full-information 783  
controller synthesis problem illustrated in Fig. 8 and let  $W_e$  be a 784  
dynamic tracking-error filter. A low-pass weight on the tracking 785  
error improves the low-frequency tracking performance, without 786  
needing to change the assumed frequency content of the reference 787

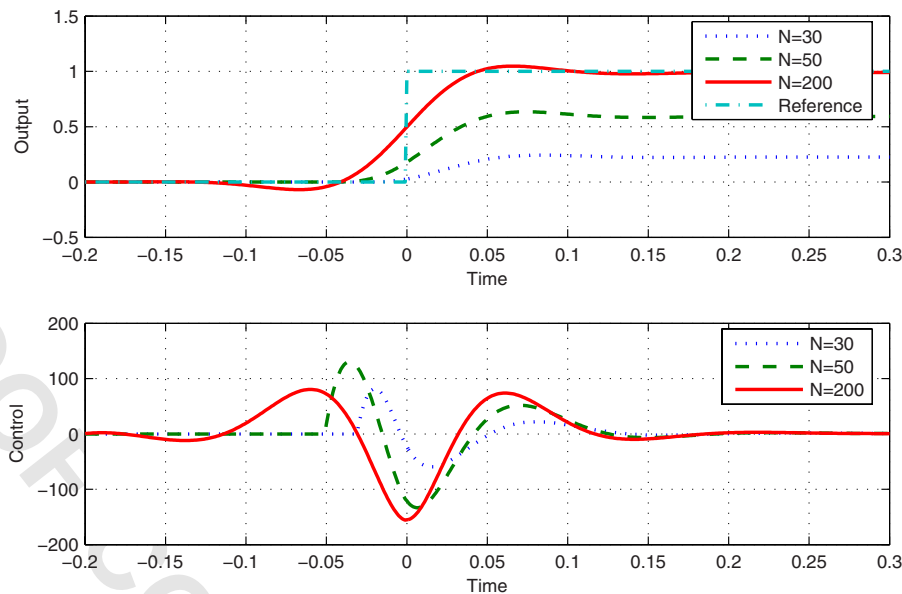


**Fig. 9** Closed-loop response of the system described in Eq. (50) and Fig. 8 with  $W_r=1$  and  $W_e=1000$ . The plotted output is the signal  $z_g$  in Fig. 8, and shows the relative nonresponsiveness of the low-preview-horizon system.

788 signal (i.e., without changing  $W_r$ ). Note that a step change in the  
789 reference does not lead to a “spike” in the control signal—see Fig.  
790 12.

791 **8.2.4 Improving the Low-Frequency Tracking Behavior.** It ap-  
792 pears that there are three alternative ways of improving the low-  
793 frequency tracking behavior, which could be used alone or in  
794 combination: (a) use a long preview horizon, (b) add a low-pass  
795 reference filter, and (c) introduce a low-pass tracking-error filter.  
796 These alternatives are illustrated in Fig. 11. In order to achieve a  
797 fair comparison,  $W_e$  was scaled so that the resulting closed loops  
798 achieved approximately similar rise times. The tracking-error fil-  
799 ter achieves good steady-state performance without excessive

control or large control spikes. However, the introduction of a  
tracking-error filter tends to introduce additional phase lag, which  
can have a deleterious effect on the loop’s robust stability. In  
contrast, the feedback part of the controller is independent of  $W_r$ ,  
which means that a reference filter can be used without jeopardiz-  
ing stability.

**8.2.5 Preview Reduces the Peak Control Magnitude.** Figure  
12 illustrates the influence of preview on the control magnitude.  
In this example, the output response is not strongly influenced by  
changes in the preview horizon, but the peak control magnitude  
reduces substantially as the preview horizon increases. This effect

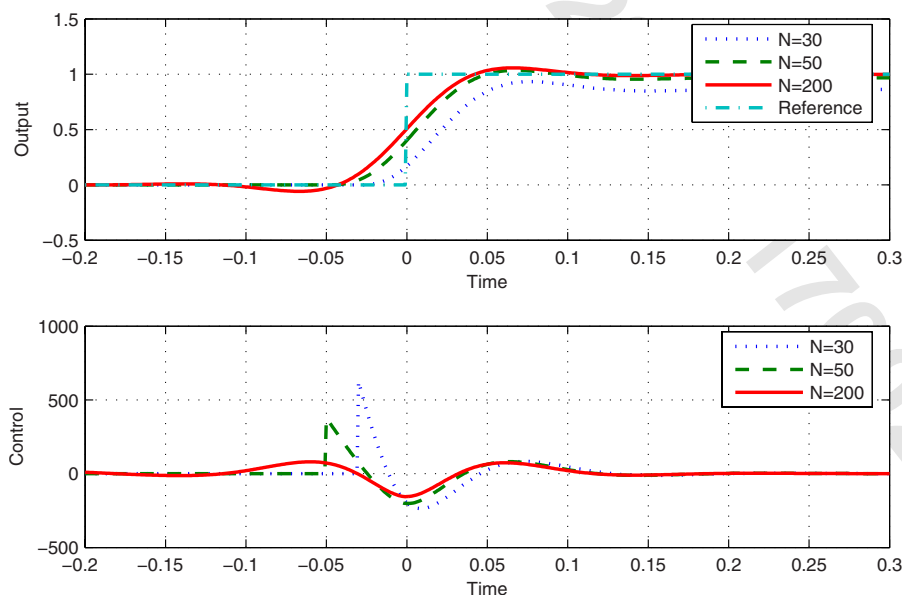


**Fig. 10** Closed-loop response of the system described in Eq. (50) and Fig. 8; the reference weight is given by  $W_r=Z/(Z-0.99)$ , with  $W_e=1000$ . The improved step response (of  $z_g$ ) for short preview horizons is clearly visible. Note the high-amplitude control in the  $N=30$  case.

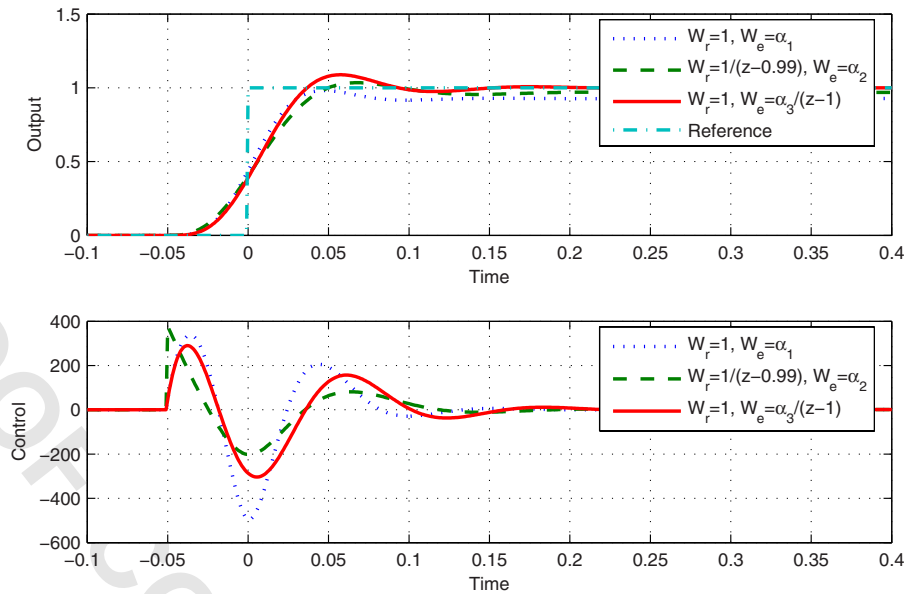


**Fig. 11** Closed-loop response of the example system described in Eq. (50) and Fig. 8. The preview horizon is fixed at  $N=50$  and  $\alpha_i$  is used to achieve similar closed-loop rise times. While the closed-loop responses ( $z_g$ ) are similar, the control signals are quite different; especially near the beginning of the preview horizon.

can be very useful in application in which control ceilings are a limiting factor, and one wishes to maintain a short rise time.

**8.2.6 Preview Only Improves Low-Frequency Tracking Performance.** For a low-pass plant, high frequency tracking performance is limited by the prohibitive amplitude of the control action. This is a fundamental feature of the plant and cannot be changed by anticipative action. This effect is illustrated in Figs. 13(a) and 13(b), where preview improves the low-frequency performance by reducing the magnitude of both the tracking error and the control signal.

**8.2.7 Integral Action With Output Feedback.** An output-feedback tracking controller with integral action is described by Fig. 14, which also serves to illustrate the complexity of problems that may be tackled using the framework in Fig. 1. Note that the integrated error signal must be included in the measurements in order to ensure that the integrator state is detectable.

Tuning the relative magnitudes of  $W_{e1}$  and  $W_{e2}$  is akin to adjusting the gains in a PI controller. In fact a derivative signal could also be added, thus completing the PID analogy and facilitating tuning of the preview controller.

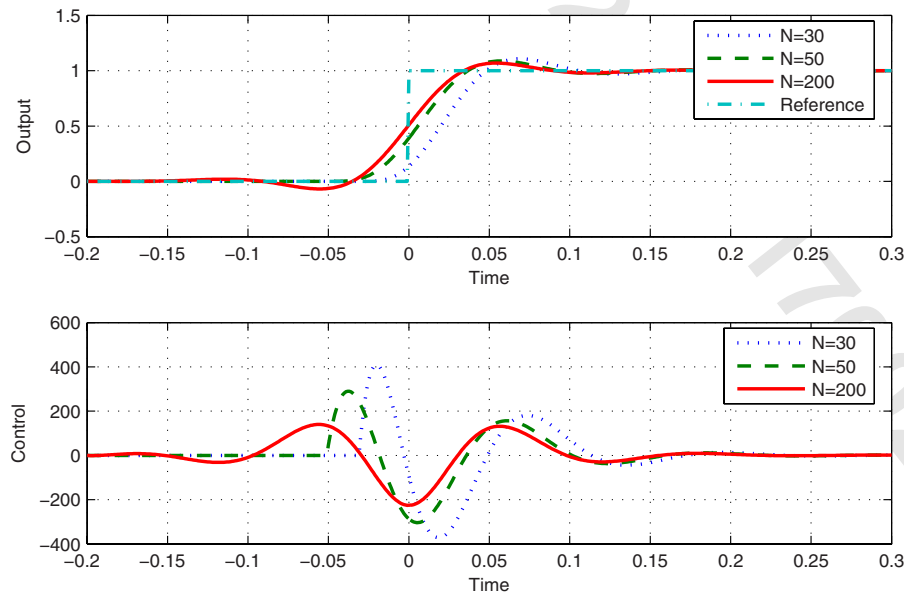


**Fig. 12** Closed-loop response of the example system described in Eq. (50) and Fig. 9; the weighting functions are  $W_r=1$  and  $W_e=100/(1-z)$ . The plotted output is the signal  $z_g$  in Fig. 8, and is relatively insensitive to the preview horizon. The control signal becomes "spread out," and lower in amplitude, as the preview horizon is increased.



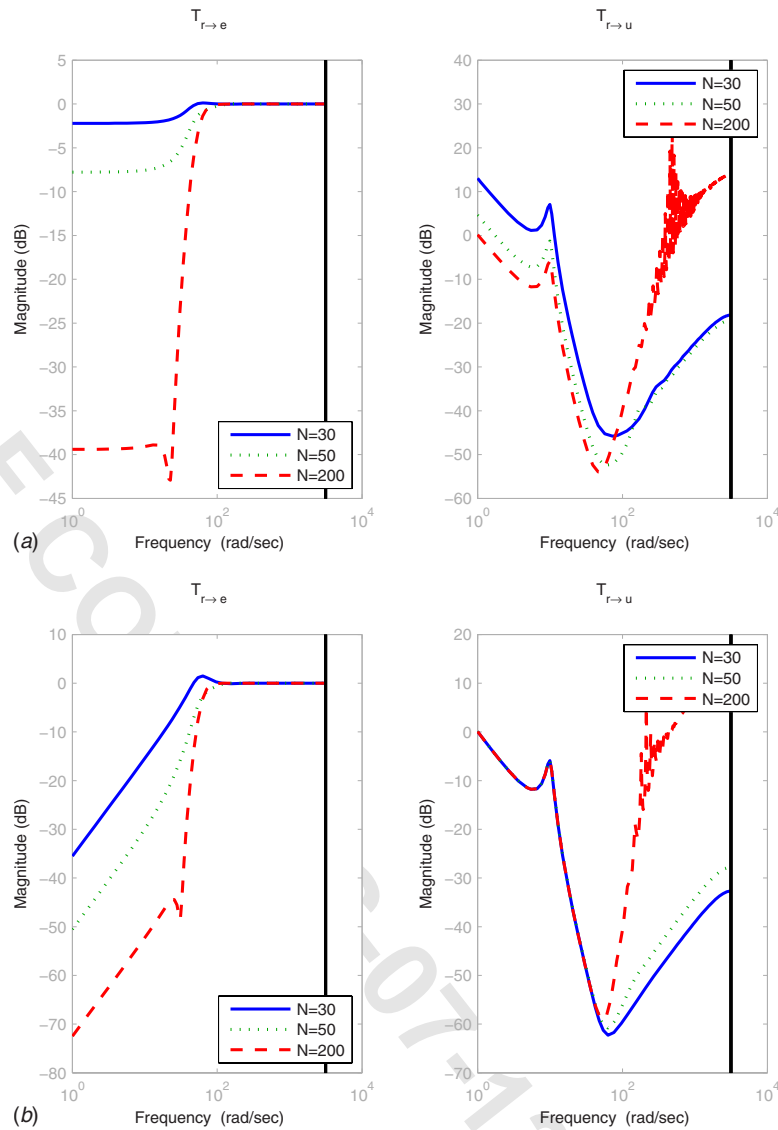


**Fig. 13** Bode plots of the closed-loop transfer functions  $T_{r \rightarrow e}$  and  $T_{r \rightarrow u}$ , which result from the application of the  $\mathcal{H}_\infty$ -optimal controls. The unweighted plant is considered in (a), and a low-pass  $W_e$  ( $W_e=1/(z-1)$ ) is employed in (b).

Previously, the addition of integral action has been approached in a LQG setting through the use of the differentiated control signal in the cost function (e.g., Refs. [7,25,8]). Such an approach

does not allow one to adjust the strength of the integral action, which is likely to lead to difficulty in satisfying stability/performance requirements.

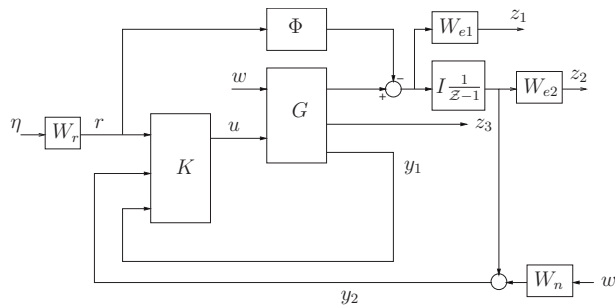


**Fig. 14** Preview tracking with integral action. The signal  $z=[z_1' z_2' z_3']'$  is the output of the closed-loop transfer function whose  $\mathcal{H}_2$ -norm is to be minimized;  $y=[y_1' y_2']'$  is the measurement signal. The transfer functions  $W_{e1}$ ,  $W_{e2}$ , and  $W_n$  are shaping filters. The other notation follows that of Fig. 1.

## 9 Concluding Remarks

Preview control has been studied for at least four decades and a large number of theoretical results can be found in the control and mechanical engineering technical literature. In many cases the theoretical developments on discrete-time  $\mathcal{H}_2$ /LQG were driven by applications problems. Contemporary applications include for example active automotive suspension control [14,13], helicopter flight control [26], and driver steering control [27]. Other applications examples, which are also related to vehicle dynamics problems, can be found in the author's thesis, Ref. [21]. A MATLAB preview control toolbox implementing the presented algorithms, together with their  $\mathcal{H}_\infty$  counterpart, is also available.<sup>2</sup>

In the authors' opinion, the strong influence of applications problems has produced a body of theory that is example-specific

<sup>2</sup><http://code.google.com/p/preview-control-toolbox/>.

and consequently somewhat restricted in terms of its scope and generality. To the best of their knowledge, a complete set of tools for synthesizing  $\mathcal{H}_2$  preview controllers that solve a broad range of realistic design problems is unavailable in the open literature. The provision of these tools is the central purpose of the work presented here. The authors present a general preview problem that captures most of the results in the contemporary literature, as well as offering a solution framework for more complex preview problems such as the preview tracking with integral action problem illustrated in Fig. 14.

The preview control problem studied in this paper is shown in Fig. 1, and it comprises a plant that is controlled by a two-degrees-of-freedom controller. The controller is synthesized to optimize the closed-loop system's response to a combination of previewable and nonpreviewable exogenous inputs. The presented solution includes an efficient computational framework that is based on two low-order Riccati equations with dimension that of the plant (excluding the preview delay line). This algorithm also includes an efficient computation of the perfect information controller gains as well as the controller itself. We have also provided an efficient method for finding the  $\mathcal{H}_2$ -norm of the closed-loop system, and a method for evaluating the norm reduction due to preview as  $N \rightarrow \infty$ . As is shown in Figs. 4 and 7, the controller structure is essentially low-order with the preview part implemented using an efficient finite-impulse-response section.

## Acknowledgment

This work was supported by a portfolio partnership held with the British Engineering and Physical Sciences Research Council (EPSRC), and also by the Flapless Air Vehicle Integrated Industrial Research program funded by BAe Systems and the EPSRC.

## References

- [1] Sheridan, T. B., 1966, "Three Models of Preview Control," *IEEE Trans on Human Factors in Electronics*, **HFE-7**(2), pp. 91–102.
- [2] Bender, E. K., 1968, "Optimal Linear Preview Control With Application to Vehicle Suspension," *ASME J. Basic Eng., Ser. D*, **90**(2), pp. 213–221.
- [3] Tomizuka, M., 1973, "The Optimal Finite Preview Problem and Its Application to Man-Machine Systems," Ph.D. thesis, Massachusetts Institute of Technology, Cambridge, MA.
- [4] Tomizuka, M., 1975, "Optimal Continuous Finite Preview Problem," *IEEE Trans. Autom. Control*, **20**(3), pp. 362–365.
- [5] Lindquist, A., 1968, "On Optimal Stochastic Control With Smoothed Information," *Inf. Sci. (N.Y.)*, **1**(1), pp. 55–85.
- [6] Tomizuka, M., and Whitney, D. E., 1975, "Optimal Discrete Finite Preview

- Problems (Why and How Is Future Information Important?)," *ASME J. Dyn. Syst., Meas., Control*, **97**(4), pp. 319–325.
- [7] Tomizuka, M., and Rosenthal, D. E., 1979, "On the Optimal Digital State Vector Feedback Controller With Integral and Preview Actions," *ASME J. Dyn. Syst., Meas., Control*, **101**(2), pp. 172–178.
- [8] Tomizuka, M., and Fung, D., 1980, "Design of Digital Feedforward/Preview Controllers for Processes With Predetermined Feedback Controllers," *ASME J. Dyn. Syst., Meas., Control*, **102**(4), pp. 218–225.
- [9] Zattoni, E., 2006, " $\mathcal{H}_2$ -Optimal Decoupling With Preview: A Dynamic Feedforward Solution Based on Factorization Techniques," *Proceedings of the 2006 American Control Conference*, IEEE, pp. 316–320.
- [10] Marro, G., and Zattoni, E., 2005, " $\mathcal{H}_2$ -Optimal Rejection With Preview in the Continuous-Time Domain," *Automatica*, **41**(5), pp. 815–821.
- [11] Tomizuka, M., 1976, "Optimal Preview Control With Application to Vehicle Suspension—Revisited," *ASME J. Dyn. Syst., Meas., Control*, **98**(3), pp. 362–365.
- [12] Hac, A., 1992, "Optimal Linear Preview Control of Active Vehicle Suspension," *Veh. Syst. Dyn.*, **21**(1), pp. 167–195.
- [13] Marzbanrad, J., Ahmadi, G., Zohoor, H., and Hojjat, Y., 2004, "Stochastic Optimal Preview Control of a Vehicle Suspension," *J. Sound Vib.*, **275**(3–5), pp. 973–990.
- [14] Roh, H. S., and Park, Y., 1999, "Stochastic Optimal Preview Control of an Active Vehicle Suspension," *J. Sound Vib.*, **220**(2), pp. 313–330.
- [15] Sharp, R. S., 2005, "Driver Steering Control and a New Perspective on Car Handling Qualities," *Proc. Inst. Mech. Eng., Part C: J. Mech. Eng. Sci.*, **219**(10), pp. 1041–1051.
- [16] Green, M., and Limebeer, D. J. N., 1995, *Linear Robust Control*, Prentice-Hall, Englewood Cliffs, NJ.
- [17] Zhou, K., Doyle, J., and Glover, K., 1996, *Robust and Optimal Control*, Prentice-Hall, Englewood Cliffs, NJ.
- [18] Doyle, J. C., Francis, B. A., and Tannenbaum, A. R., 1990, *Feedback Control Theory*, Macmillan, New York.
- [19] Middleton, R. H., Chen, J., and Freudenberg, J. S., 2004, "Tracking Sensitivity and Achievable  $\mathcal{H}_\infty$  Performance in Preview Control," *Automatica*, **40**(8), pp. 1297–1306.
- [20] Houpis, C. H., and Lamont, G. B., 1991, *Digital Control Systems*, 2nd ed., McGraw-Hill, New York.
- [21] Hazell, A. J., 2008, "Discrete-Time Optimal Preview Control," Ph.D. thesis, Imperial College, London, <http://deposit.dpot.edina.ac.uk/145/>
- [22] Moelja, A. A., and Meinsma, G., 2006, " $\mathcal{H}_2$  Control of Preview Systems," *Automatica*, **42**(6), pp. 945–952.
- [23] Hazell, A. J., and Limebeer, D. J. N., 2008, "An Efficient Algorithm for Discrete-Time  $\mathcal{H}_\infty$  Preview Control," *Automatica*, **44**(9), pp. 2441–2448.
- [24] Anderson, B. D. O., and Moore, J. B., 1979, *Optimal Filtering*, Prentice-Hall, Englewood Cliffs, NJ.
- [25] Katayama, T., and Hirono, T., 1987, "Design of an Optimal Servomechanism With Preview Action and Its Dual Problem," *Int. J. Control*, **45**, pp. 407–420.
- [26] Paulino, N., Cunha, R., and Silvestre, C., 2006, "Affine Parameter-Dependent Preview Control for Rotorcraft Terrain Following Flight," *J. Guid. Control Dyn.*, **29**(6), pp. 1350–1359.
- [27] Cole, D. J., Pick, A. J., and Odhams, A. M. C., 2006, "Predictive and Linear Quadratic Methods for Potential Application to Modelling Driver Steering Control," *Veh. Syst. Dyn.*, **44**(3), pp. 259–284.

AUTHOR QUERIES — 017002JDS

- #1 Author: Please verify fonts throughout the article.

PROOF COPY [DS-07-1223] 017002JDS